Ollscoil na Gaillimhe
University of Galway

Extremely low-cycle fatigue testing of structural carbon steel for a novel self-centring system

Title	Extremely low-cycle fatigue testing of structural carbon steel for a novel self-centring system
Author(s)	Alwahsh, Hatim;Salawdeh, Suhaib;Jiang, Yadong;Goggins, Jamie
Publication Date	2024-08-29
Publisher	Civil Engineering Research Association of Ireland

Extremely Low-cycle Fatigue Testing of Structural Carbon Steel for a Novel Self-Centring System

H. Alwahsh[1], S. Salawdeh[2], Y. Jiang[1], J. Goggins[1,3]

[1] SFI MaREI Research Centre, Ryan Institute, School of Engineering, University of Galway, Galway, Ireland
[2] Department of Building & Civil Engineering, Atlantic Technological University, Galway, Ireland
[3] Construct Innovate, University of Galway, Galway, Ireland
email : H.alwahsh1@ universityofgalway.ie, Suhaib.Salawdeh@atu.ie, yadong.jiang@universityofgalway.ie
*Corresponding author email: ***jamie.goggins@universityofgalway.ie***

ABSTRACT: In this study, laboratory experiments have been conducted in order to investigate the material behaviour of cold-form square hollow section bracing members under monotonic tensile loading and low-cycle fatigue loading. Two different materials, namely S275 and S235, were tested at room temperature. The tested coupons were cut from the bracing members of a novel concentrically braced self-centring frame. The low- and extremely low- cycle fatigue tests were performed at various strain amplitudes. Cyclic hardening and cyclic softening to different strain amplitudes are studied to find material properties. The buckling and Bauschinger effects in the specimens seemed to have an impact on the results. From the tensile test results, the mechanical properties of the specimens such as ultimate tensile strength, yield strength, percentage of elongation and area reduction, fracture strain and young's modulus were derived. In addition, the parameters for a mixed strain hardening model of isotropic and kinematic are determined from each hysteresis loop with different strain amplitudes. The strength and ductility hardening parameters were calibrated for the Coffin-Mason relationship. The comparison between the experimental results and calibrated material model showed a good agreement. The obtained test results and material model provides important data for the performance analyses of the self-centring structures.

KEY WORDS: Mechanical properties, Coupon test, uniaxial tensile test, low-cycle fatigue, cyclic loading

1 INTRODUCTION

Generally, the earthquake-resistant design relies on nominal static properties of materials, such as the nominal yield strength of structural steel. However, in order to perform realistic assessment for the resilience of the structure when subjected to quake-induced cyclic loading, such as fatigue-induced failure, the nominal materials properties provide no insight into the real response of the structure during earthquakes. Hysteresis and hardening behaviour of the structural steel provide better insight into the over-strength factor of the yield and ultimate strength of the metal, which is very useful for economising the earthquake-resistant design. Combining the fatigue and stress-life behaviour of the metal helps improve sustainable design of the structure and the predictability of its realistic life span under cyclic loading.

The behaviour of steel elements under cyclic loads is significantly important in terms of earthquake loading. The cyclic behaviour of steel elements reveals much more information or data about the deterioration of the structure due to the comparison of reversal deformations with monotonic loadings [1-3]. The mechanical properties are critical for the evaluation of the behaviour of the structural elements. For the seismic design and material parameters, the mechanical properties are usually found in a series of international standards. For instance, BS 10002, ASTEM E8/E8M, ISO 6892-1 [4-6]. In general, the key material parameters in seismic design and materials' development are not limited to static material properties. Dynamic characteristics are also important part of the fundamental mechanical properties of the materials. Therefore, mechanical properties and fatigue analysis are the most crucial criteria which affect the sound design and evaluation of the structural elements.

The current research focuses on monotonic and low-cycle fatigue tests to evaluate the mechanical properties of steel necessary for tracing the performance of the structural systems under seismic loading. The quasi-static tensile test and constant strain amplitude cyclic tests are presented. The results will be used to develop strain-life relationships and cyclic hardening parameters, suitable for incorporation into numerical models to predict the fracture of structural members that are subjected to large amplitude cyclic loading that may result from severe earthquakes.

2 METHODOLOGY

Figure 1 summarises the methodology of this study. A total of 30 tensile coupons and 48 cyclic loading specimens were tested. The coupons were machined from 4 mm, 3 mm, 2.5 mm thick bracing members (square hollow section (SHS)) and 4 mm and 6 mm thick gusset plates. Figure 2(a) illustrates the geometrical details of the specimens. Figure 2 (b) depicts the location of the machined coupons which extracted from the flat faces of square hollow sections opposite to the welded side.

The monotonic tensile tests comprised a total of 20 coupons, categorised across four sections of SHS bracing. Additionally, there were 10 tensile tests conducted specifically on gusset plates. The monotonic tensile tests were performed according to European standard ISO 6892-1 [5] for the SHS and ASTM E8/E8M [6] for gusset plate. A good representation of fatigue-life curve requires at least 12 valid tests to accurately determine the curve shape and estimate the material statistical scatter. Increasing the number of specimens increases the confidence level.

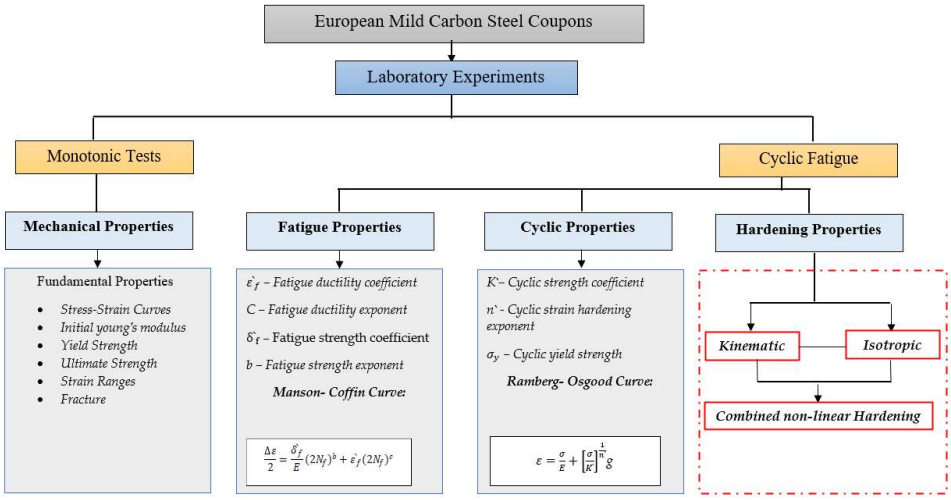

Figure 1. Flowchart of the methodology for the tensile and fatigue tests.

In order to cover both the elastic and the plastic ranges of behaviour, tests were conducted under five different strain amplitudes under a range of universal standards provided by European and American professional societies [7, 8]. The low-cycle fatigue (LCF) and extremely low-cycle fatigue (ELCF) are of most importance due to its relevance to earthquake engineering. The most common method for predicting the low-cycle fatigue life of metals is the Coffin-Mason relationship [9].The strain life data could be presented as linear relationship on log-log scale, these parameters are important for the material numerical modelling [10, 11].

The expected data from the tests are loads, loading head displacements, and strain of the coupon. The loads and the displacements of the loading head were recorded internally by the Instron testing system. There were strain gauges installed at the middle of the coupon gauge length. The uni-axial strain gauges used in the tests have a gauge length of 5 mm and a strain limit of 5%. However, the maximum strain of the coupons in the monotonic tensile tests were generally larger than 5%.

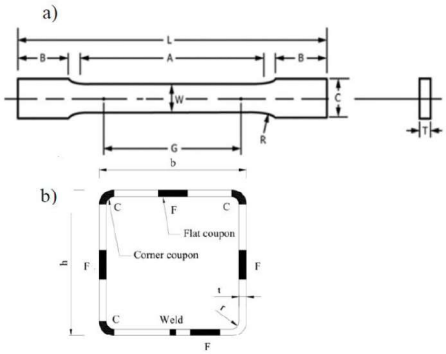

Figure 2. a) Nominal dimensions of monotonic and fatigue tests specimen standards b) Location of flat and curved coupon of hollow sections elements [12].

Hence, the digital image correlation (DIC) technology was applied to extract strain measurements when the strain gauges were out of range. On one side of the coupon, black speckle pattern was painted. A camera was set up in front of the steel coupon to record the images of the deformed speckle pattern.

The label of each coupon is based on the reference point of the gusset plate. For SHS coupons, the label (e.g., S1-1-1-A-1) indicates the specimen, location, and number of the coupons. The letters A, B, and C denote the side from which the coupon was cut: A is the opposite side of the welded side, B is counterclockwise, and C is clockwise. The last number indicates the position of the coupon relative to the reference point, with 1 being the nearest and increasing sequentially for up to three coupons.

3 EXPERIMENTAL RESULTS AND DISCUSSION

3.1 Monotonic Tensile Tests Results

The results of the tests on each sample of material as obtained from the data are important because they give significant information about the static mechanical properties of the materials, which are necessary for modelling. The summary of measured and computed mechanical properties resulted from the tested specimens are illustrated in Table 1. This table provides the average values for the results of the specimens taken from the bracings members and gusset plates for the two types of steel grades S235 and S275. The stress-strain results obtained for each steel grade from monotonic tests for some specimens are presented in Figure 3. As a primary result, the stress-strain curves seem to be highly sensitive to the dimensions of the specimens, even for the same type of steel.

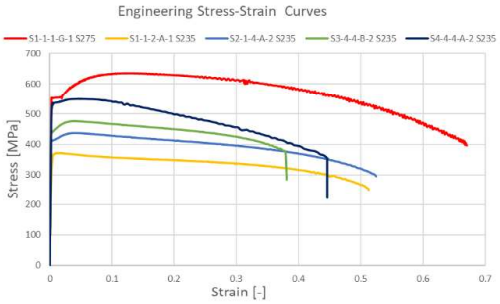

Figure 3. Stress-strain curve under uniaxial tensile loading

Results show that there is some variation in the resulting stress-strain curves for the same grade of steel. For instance, for the steel grade (S235), specimen S4-4-4-A-2 was the highest value for braces. In general, the smaller the thickness of the specimen, the smaller the strength as shown in the stress-strain curve. For gusset plates made from S275 steel, specimen S1-1-1-G-1 had the highest yield strength.

Table 1. The summary results of the major monotonic tensile materials parameters.

Brace coupon	Steel Grade	$R_p(f_y)$ (N/mm^2)	$R_m(f_u)$ (N/mm^2)	E (N/mm^2)
40x40x4	S235	355	375	182020
30x30x3	S235	417	442	208388
25x25x2	S235	441	476	204975
20x20x3	S235	535	549	205996
Mean	-------	437	460	200344
S. D	-------	74	72	12300
COV (%)	-------	17	160	6
Plate coupon	Steel Grade	$R_p(f_y)$ (N/mm^2)	$R_m(f_u)$ (N/mm^2)	E (N/mm^2)
S 40-G	S275	544	634	212872
S 30-G	S275	266	332	210703
S 25-G	S275	292	344	205751
S 20-G	S275	257	339	193102
Mean	-------	340	412	205048
S. D	--------	136	148	8912
COV (%)	--------	40	36	4.35

E: Young's Modulus,
$R_p(f_y)$: Yield Strength
$R_m(f_u)$: Ultimate Tensile Strength

3.2 Low-Cycle Fatigue Test Results

3.2.1 Cyclic Hardening & Softening

Cyclic softening and cyclic hardening are associated with the decreasing and increasing resistive behaviour of the materials against permanent deformations. There are different ways to represent the fatigue life, ranging from uniaxial model to multiaxial constative models. This study adopted uniaxial testing for fatigue characterisation due to its simplicity. Knowing the trend and features of cyclic behaviour is critical for better understanding of the steel behaviour during the earthquake excitation.

In this study, the specimens were tested at different strain amplitudes (±0.5%, ±1%, ±2%, ±3% and ±5%). Overall results demonstrate typical cyclic softening behaviour for a given strain amplitude. This trend of behaviour might be due to the rolling process in the manufacturing phase of the members. For instance, Figure 4 illustrates the cyclic softening behaviour of the S1-1 coupon material under strain amplitudes of 1% and 3%, respectively. The figure also compares these cyclic responses to the results of a monotonic tensile test. As can be seen, the cyclic strains result compared to the monotonic loading test.

3.2.2 Establishing hardening parameters

The cyclic Ramberg-Osgood stress-strain parameters can be derived using the experimental cyclic stress-strain curves by tracing the peak values of the stresses of the stabilised loops per strain amplitude. For each strain amplitude, the stabilized stress-strain loop was chosen as the hysteresis loop at half the number of cycles experienced before failure. A plot relating the various strain amplitudes to their corresponding stress amplitudes is typically used to determine the cyclic strength coefficient (K') and cyclic strain hardening exponent (n').

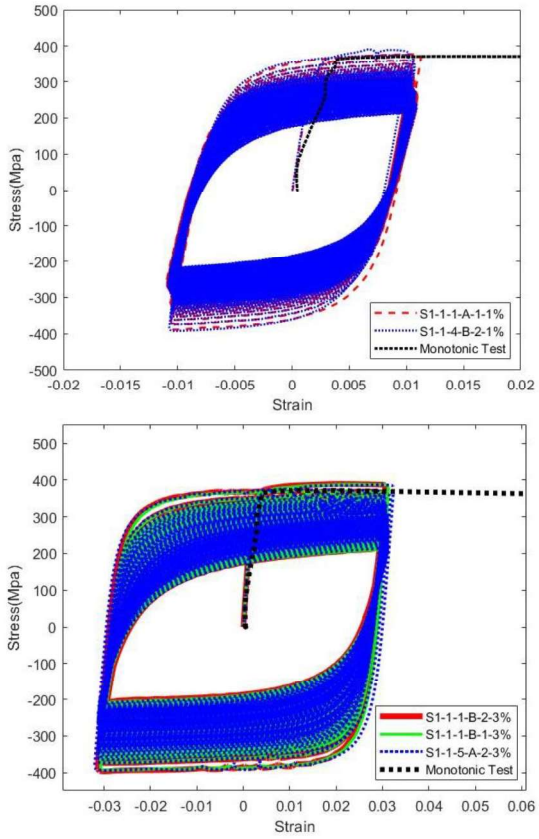

Figure 4. Comparison between cyclic and monotonic results specimens a) S1-1-1% b) S1-1-3%

3.2.3 Strain-Life Relationship Results

The LCF and ELCF data are represented by constant strain amplitudes cyclic coupon tests in this research for targeted coupon sections. The plastic strain-life relationship based on the LCF regime, which is known as Coffin-Manson relationship is presented as the expression in Eq 1. The progress of the stress at each strain amplitude illustrates the rate and the variation of the cyclic hardening. This curve is a function of stress amplitude and number of cycles.

$$\frac{\Delta\varepsilon_p}{2} = \varepsilon_f^{'}(2N_f)^c \quad (1)$$

ε_f': Fatigue ductility coefficient
c : Fatigue ductility exponent
ε_p : Fatigue strength coefficient
$2N_f$: Number of reversals to failure

The material behaviour generally stabilises quite rapidly, as shown by the stress and strain measurements. Figure 5 depicts the measured load during the initial cycles of a representative test at a constant strain amplitude. Figure 6, on the other hand,

shows the relationship between the number of cycles and the applied strain. These figures together demonstrate the stabilisation of the material's behaviour during the cyclic loading process. As can be seen, the stress and strain amplitudes, as reflected in the load measurements, reach a stable value after a few numbers of cycles.

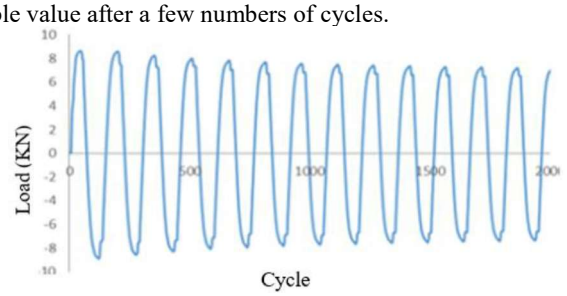

Figure 5. Measurement of load during a typical test at 1% amplitude (SHS 40x40)

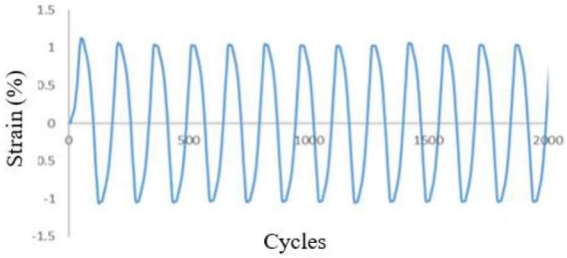

Figure 6. Measurement of strain during the first few cycles of a typical test at 1% amplitude (SHS 40x40)

The resulting parameters of the Coffin-Manson relationship are defined in Table 2 based on the above-mentioned procedure. Figure 7 below illustrates the Coffin-Manson relationship for the different tubular group sections. As indicated in Table 2, the values of ductility coefficient (ε'_f) were not significantly close to each other, around 0.24 for SHS 40x40 section and nearly 0.68 for section 30x30. The values of SHS sections 25x25 and 20x20 were almost equal 0.1. The values of the COV varied significantly for both tests (cyclic and monotonic). It is worth noting that the COV was relatively high for the fatigue ductility coefficient, this is due to the high value of the specimen 30x30, and if we exclude this value, the COV drops to 42%. Similarly, the COV of the fatigue ductility exponent decreases to 6 %.

Table 2. Coffin-Manson law and Ramberg-Osgood parameters.

Specimen ID	Fatigue ductility coefficient, $\boldsymbol{\varepsilon_f}'$(%) (Plastic Range)	Fatigue ductility exponent, c (Plastic Range)	Fatigue Strength coefficient, $\boldsymbol{\sigma_f}'/\boldsymbol{E}$(%) (Elastic Range)	Fatigue Strength exponent, b (Elastic Range)
40x40x4.0	0.240	-0.441	0.0704	-0.548
30x30x3.0	0.678	-0.648	0.0407	-0.466
25x25x2.5	0.100	-0.478	0.0085	-0.234
20x20x3.0	0.104	-0.409	0.004	-0.070
Mean	0.280	-0.494	0.031	-0.329
STD	0.236	0.092	0.026	0.188
COV	84.26	-18.66	86.86	-57.35

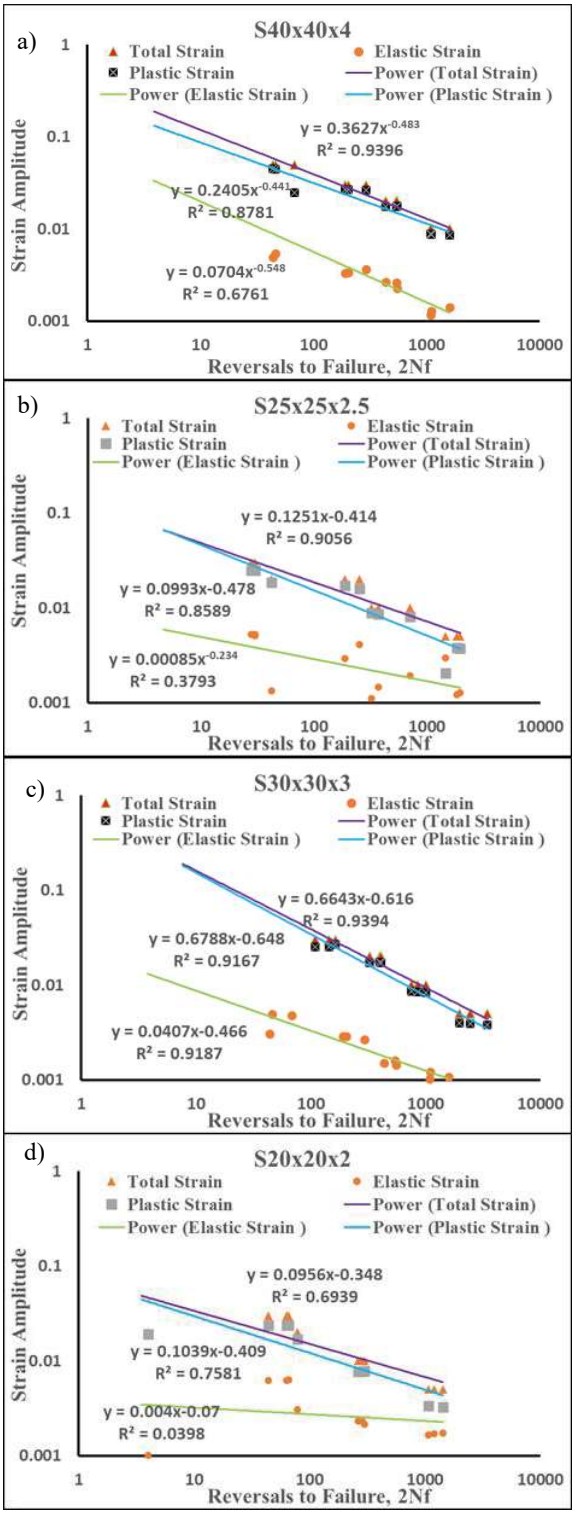

Figure 7. Strain-life relationship in the LCF regime a) SHS 40x40 tubular section b) SHS 30x30 tubular section c) SHS 25x25 tubular section d) SHS 20x20 tubular section

3.2.4 Cyclic material hardening model calibration

Experimental data and MATLAB [13] simulated model of stress strain hysteresis curves of cold-formed carbon steel from the first cycle to the half-life cycle at various strain amplitude

tests are shown in Figure 8. The least squares regression fitting procedures was used to extract the combined hardening parameters and to calibrate between the analytical and experimental data. The results indicate that the fitted cyclic model is capable of capturing the experimental hysteresis features. As can be seen from graphs below, the trend of the cyclic behaviour has softening during the half number of cycles to failure of the tests.

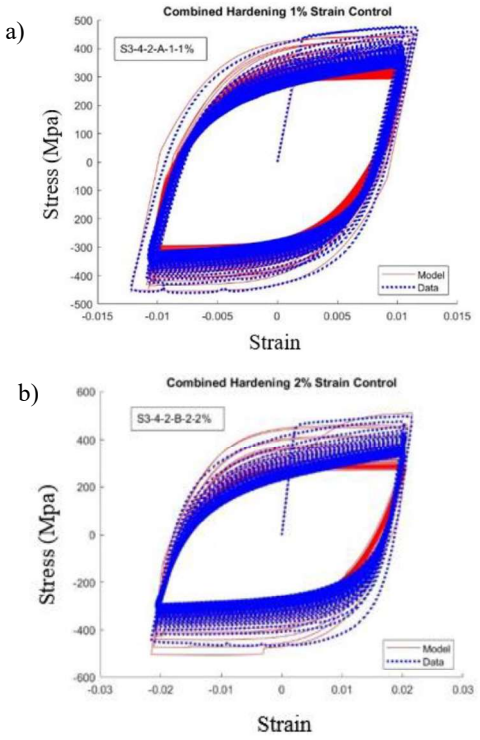

Figure 8. Experimental and simulated stress-strain curves under different strain amplitude tests a) S3-4-1% b) S3-4-2%

Figure 9 compares the stress-strain response of cold-formed carbon steel during the first 3 cycles of a 1% strain amplitude test. The figure includes both experimental data and a MATLAB simulation of the hysteresis curves. The model curves have been fitted through minimising the sum of the squares of the errors between the model and the data with a goodness of fit (R^2 = 0.99). These results show consistency pattern between both experiments and simulations as shown in most curves (See Figure 8).

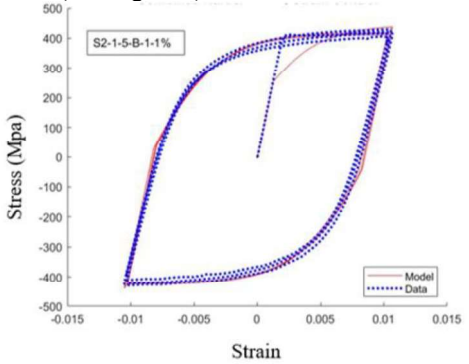

Figure 9. Stress-strain curves at the first three cycles of 1% strain amplitude test (25x25x2.5 brace).

3.3 Failure Mode

The tensile failure mode shows typical necking failure at the region of uniform width. Some samples have grip failure owing to absence of the hourglass gauge length due to limited dimensions of the tested coupons. As can be seen from Figure 10, there are different failure locations and modes. It is worth mentioning that most of the specimens have ductile fracture behaviour. Stress-strain curves at the first three cycles of 1% strain amplitude test (25x25x2.5 brace). It can be noticed from the axial experimental data that the softening governs the behaviour of the materials. The results reveal that some specimens exhibit buckling effects at high strain amplitudes, as shown in Figure 10 As a general observation, the smaller the thickness of the specimen, the more the buckling effects show up.

Also, as reported by other researchers [14], the manufacturing process has an influence on the softening of the cyclic stress-strain curves of steels. The Bauschinger effect is clearly observed in some of the tests. It is worth mentioning that the specimens in the current study were taken from bracing members that have been strained beyond yield points in the shaking table tests. Thus, previous strain hardening of the specimens may have an influence on the softening of the cyclic stress-strain curves. Figure 10 depicts the tensile test setup and the corresponding specimen, while Figure 11 illustrates the fatigue testing machine and its associated sample.

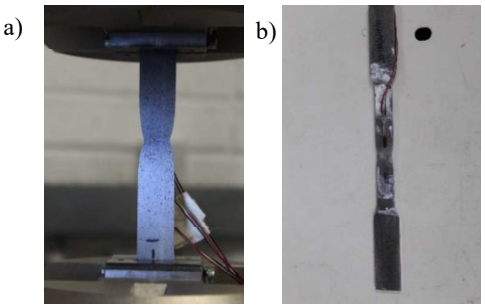

Figure 10. Necking failure mode of the specimens due to tensile test. a) S1-1-4-C-1 b) S2-1-4-A-2

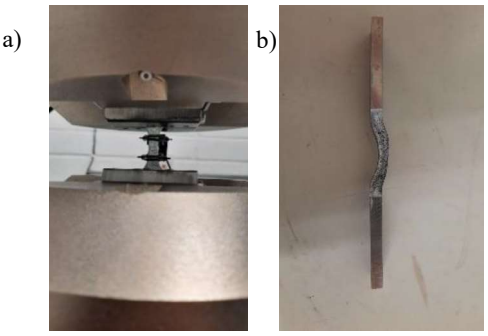

Figure 11. Buckling failure mode of the specimens due to axial fatigue test. a) S1-1-4-C-2 b) S1-1-4-C-2

It can be noticed from the low-cycle fatigue experimental data; the softening hardening govern the behaviour of the materials. The results reveal that the steel behaviour exhibits significant buckling effects at high strain amplitudes. The Bauschinger effect is clearly observed in most tested data

results. Figure 11 shows the buckling failure mode on the specimen. As a conclusion from the results, as the sections of the coupons go to small thickness, the failure controlled by buckling mode. In general, the coupons are prone to buckling failure under high strain amplitudes.

4 SUMMARY AND CONCLUSION

This research focuses on monotonic and low-cycle fatigue tests to evaluate the mechanical properties of steel, which are crucial for assessing the performance of structural systems under seismic loading. The study includes quasi-static tensile tests and constant strain amplitude cyclic tests. The results will be used to develop strain-life relationships and cyclic hardening parameters. These parameters are suitable for incorporation into numerical models to predict the fracture of structural members subjected to large amplitude cyclic loading, as may occur during severe earthquakes. Interestingly, while fatigue ductility values closely align with those reported in previous studies, fatigue strength exhibits significant variability across different research findings. More information can be found in the comprehensive steel property data presented in the materials report provided by the University of Galway. This report offers valuable insights for a wide range of future applications and research endeavours, with the potential to significantly advance the field of materials science and engineering.

Tests were conducted on both fatigue steel coupons and tensile coupons to determine the mechanical and fatigue material properties of the steel braces and gusset plates from a full-scale frame that had previously experienced earthquake excitation. A total of 48 fatigue steel coupons and 30 tensile coupons were subjected to testing under various strain rates and loading protocols, including monotonic tensile loading and cyclic straining at different strain amplitudes ranging from ±0.5% to ±5%, all performed at room temperature. The test data are used to fit a set of numerical models concerning the cyclic and fatigue material behaviour of structural steel. The results of the monotonic and the fatigue tests are summarised in the following points:

- The average Young's Modulus, yield strength, and ultimate tensile strength of the steel coupons are 202 GPa, 406 MPa, 448 MPa and the corresponding coefficient of variation (COV) are 8.7 %, 24%. 22%, respectively.
- The waveform of the fatigue test was sinusoidal, and all fatigue tests were conducted under constant frequency and constant strain amplitude, with a strain ratio of R=-1, fully reversed.
- A comparison of monotonic hardening and first-cycle hardening parameters shows that the curves are comparable and reliable.
- For the fatigue tests the average number of cycles to failures are 26, 65, 151, 397, and 1143 for 5%, 3%, 2%, 1%, and 0.5%, respectively.
- Softening behaviour was observed during cyclic tests under fixed strain amplitude. However, when comparing cyclic tests for different strain amplitudes, hardening was evident. The values for strain hardening parameters obtained over various strain amplitude vary from K' = 298 MPa, n' = 0.009 to K' = 493, n' = 0.08.
- The fatigue ductility coefficient ε'_f and the fatigue ductility exponent c are obtained using the Coffin–Manson law and cyclic stress–strain curve. The values ranged from 0.1 to 0.67 for ε'_f and -0.41 to -0.64 for c with averaged values of 0.28 and -0.494, respectively.
- The ductile fracture mode governed the tensile failure of most of the tested specimens.
- Concerning the fatigue failure mode, buckling was noticed in some of the specimens, particularly at high strain amplitudes.

ACKNOWLEDGEMENTS

This research was funded by the Seismology and Earthquake Engineering Research Infrastructure Alliance for Europe (SERA-H2020-INFRAIA-2016-2017/H2020 INFRAIA-2016-1) under grant agreement No. 730900 for the project "Investigation of Seismic Deformation Demand, Capacity and Control in a Novel Self-Centring Steel Braced Frame (SC-CBF)." The first author acknowledges the support of Science Foundation Ireland through the Career Development Award programme (Grant No. 13/CDA/2200) and the MaREI Centre (Grant No. 12/RC/2302_2). This research was also supported by the Marine Institute, funded under the Marine Research Programme by the Government of Ireland (PDOC/21/03/01).

REFERENCES

[1] ISO 12106(E). *Metallic materials-fatigue testing-axial-strain-controlled method, Geneva*. Switzerland, 2003.
[2] ASTM E606/E606M. *Standard practice for strain-controlled fatigue testing, ASTM International*. West Conshohocken, Pennsylvania, USA. , 2019.
[3] William D, Calliste J. *Materials science and engineering an introduction*: John Wiley and Sons, 2007.
[4] BS EN 10002-1. *Metallic materials _ Tensile testing _ Part 1: Method of test at ambient temperature*, 2001.
[5] *EN ISO 6892-1. Metallic materials – Tensile testing – Part 1: Method of test at ambient temperature. 2019. 6*.
[6] *E8/E8M-13a.Standard Test Methods for Tension Testing of Metallic Materials, ASTM International, West Conshohocken, PA*, 2013.
[7] ISO12106(E). *Metallic materials-fatigue testing-axial-strain-controlled method,* . Geneva. Switzerland 2003., 2003.
[8] ASTM. *E606/E606.Standard Test Method for Strain-Controlled Fatigue Testing*, 2019. Vol. 3.
[9] BS EN 10025-2:2004. Hot rolled products of structural steels. Technical delivery conditions for non-alloy structural steels. In: *BSI*. 2004:38.
[10] Radonovich D, Gordon AP. *Methods of extrapolating low cycle fatigue data to high stress amplitudes*, 2008. Vol. 43154.
[11] Rodríguez Sánchez I. (2019) Properties of steel applied in civil engineering industry in selected countries: S235 and S355.
[12] Wang J, Afshan S, Schillo N, Theofanous M, Feldmann M, Gardner L. (2017) Material properties and compressive local buckling response of high strength steel square and rectangular hollow sections. *Engineering Structures*. 130: 297-315.
[13] Higham DJ, Higham NJ. *MATLAB guide*: SIAM, 2016.
[14] Hassan T, Kyriakides S. (1992) Ratcheting in cyclic plasticity, part I: uniaxial behavior. *International journal of plasticity*. 8(1): 91-116.